

# The mathematics of burger flipping

Jean-Luc Thiffeault

<sup>a</sup>*Department of Mathematics University of Wisconsin – Madison 480 Lincoln Dr. Madison WI 53706 USA*

---

## Abstract

What is the most effective way to grill food? Timing is everything, since only one surface is exposed to heat at a given time. Should we flip only once, or many times? We present a simple model of cooking by flipping, and some interesting observations emerge. The rate of cooking depends on the spectrum of a linear operator, and on the fixed point of a map. If the system has symmetric thermal properties, the rate of cooking becomes independent of the sequence of flips, as long as the last point to be cooked is the midpoint. After numerical optimization, the flipping intervals become roughly equal in duration as their number is increased, though the final interval is significantly longer. We find that the optimal improvement in cooking time, given an arbitrary number of flips, is about 29% over a single flip. This toy problem has some characteristics reminiscent of turbulent thermal convection, such as a uniform average interior temperature with boundary layers.

---

*Dedicated to Charlie Doering, a man who appreciated a good burger and good company.*

## 1. Introduction

What is the best strategy for grilling a steak, a burger, or a slice of eggplant on a hot grill? Only one side is hot at a time, so timing is crucial. One school of thought is that flipping only once leads to more even cooking. Kenji López-Alt from The Food Lab reports on this [3]:

As food scientist and writer Harold McGee has pointed out, flipping steak repeatedly during cooking can result in a cooking time about 30% faster than flipping only once. The idea is that with repeated flips, each surface of the meat is exposed to heat relatively evenly, with very little time for it to cool down as it faces upwards. The faster you flip, the closer your setup comes to approximating a cooking device that would sear the meat from both sides simultaneously.

This raises the intriguing possibility of making a mathematical model that demonstrates this potential faster cooking. Though our model will be very simple, its simplicity will allow us to isolate the mathematical elements that induce faster cooking, opening the way to optimization.

As the simplest possible model, we take the food to be an infinite slab and only keep track of its temperature in the vertical direction. We solve the standard heat equation in that slab. Though we do not include more complicated aspects such as moisture and fat content, we do allow for imperfect conductor boundary conditions at the top and bottom of the food. Once we understand this very basic problem, we allow for a flip of the food — that is, we turn over the food on the heating surface. Mathematically, we overturn the vertical temperature distribution and allow the heat equation to act, using the flipped profile as an initial condition. We can express the flipping-and-heating operation as a map acting on the Fourier coefficients of the solution. We will see that understanding the fixed point and the spectral properties of this map is crucial to optimizing the total cooking time.

The outline of the paper is as follows. In Section 2 we introduce the model system and discuss relevant physical parameter values and our dimensionless scalings. In Section 3 we provide a solution to the simple one-dimensional model, in the form of a sum over separated solution using Sturm–Liouville theory. This is elementary, but we briefly

---

*Email address:* `jeanluc@math.wisc.edu` (Jean-Luc Thiffeault)

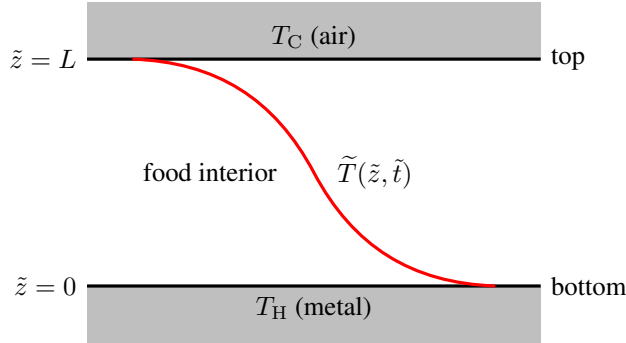


Figure 1: Slab geometry for the food. In general  $\tilde{T}(0, \tilde{t}) < T_H$  and  $\tilde{T}(L, \tilde{t}) > T_C$ , with equality only for perfect conductors.

give the details for the sake of completeness. Section 4 is devoted to the simplest cooking problem: how long does it take for the food to cook if it is never flipped? Depending on the boundary conditions, the food might never actually cook in this configuration. In Section 5 we finally add nontrivial dynamics: we flip the food at prescribed periodic times and examine the interior temperature. We define the *flip-heat operator*, which is a composition of a flip followed by a cooking interval. Section 6 treats the symmetric limit where the food has identical thermal properties at the top and bottom, which allows for further analytic progress (this is the Boussinesq limit in thermal convection [10]). We answer the burning question of optimal cooking times in Section 7: what is the optimal sequence of flips to achieve fastest cooking? Most of the results of this section are numerical; the evidence suggests that the problem has a unique global minimum. We offer some concluding remarks in Section 8.<sup>1</sup>

## 2. The model equations and physical parameters

We consider a piece of food that is relatively flat and thin, being cooked on a heating surface, and that can be turned over — flipped — to assist cooking. We model the food as an infinite slab, extending from  $\tilde{z} = 0$  to  $\tilde{z} = L$  in the vertical (see Fig. 1). In dimensional form, the temperature  $\tilde{T}(\tilde{z}, \tilde{t})$  in the food satisfies the heat equation

$$\tilde{T}_{\tilde{t}} = \kappa \tilde{T}_{\tilde{z}\tilde{z}}, \quad 0 < \tilde{z} < L, \quad \tilde{t} > 0, \quad (2.1a)$$

with initial condition

$$\tilde{T}(\tilde{z}, 0) = \tilde{T}_0(\tilde{z}). \quad (2.1b)$$

(The subscripts  $\tilde{t}$  and  $\tilde{z}$  denote partial derivatives.) Newton's law of cooling gives the boundary conditions [6, p. 7]

$$-k \tilde{T}_{\tilde{z}}(0, \tilde{t}) = \tilde{h}_0 (T_H - \tilde{T}(0, \tilde{t})), \quad k \tilde{T}_{\tilde{z}}(L, \tilde{t}) = \tilde{h}_1 (T_C - \tilde{T}(L, \tilde{t})), \quad (2.1c)$$

where  $\tilde{h}_0 > 0$  and  $\tilde{h}_1 \geq 0$ , in order that heat flow obeys the second law of thermodynamics. For  $\tilde{h}_i \rightarrow \infty$  we recover a perfect conductor (fixed-temperature boundary condition), and for  $\tilde{h}_1 = 0$  we have a perfect insulator, which we disallow at the heating surface ( $\tilde{h}_0 > 0$ ).

The physical constants involved can vary wildly for different types of food and cooking surfaces, and for simplicity we will mostly confine ourselves to one set of parameters as listed in Table 1, unless otherwise noted. For a meat patty, we get physical parameters from Zorrilla and Singh [11] (see also [7]). At the bottom, they use a ‘contact heat transfer coefficient’  $h_0 = 900 \text{ W/m}^2 \text{ }^\circ\text{C}$  at the interface of the heating surface and the meat ( $\tilde{z} = 0$ ) [11, p. 62], which lumps together the resistance of a thin layer of fat, air, and moisture. At the top, they take a combined radiation and convection heat transfer coefficient  $h_1 = 60 \text{ W/m}^2 \text{ }^\circ\text{C}$ . In the interior of the food, they use a thermal conductivity

<sup>1</sup>Throughout the paper, footnotes indicate when a particular MATLAB script can be used to reproduce a computation. The code can be downloaded on [https://github.com/jeanluct/cookflip\\_code](https://github.com/jeanluct/cookflip_code).

$k = 0.416 \text{ W/m}^\circ\text{C}$ . The volumetric heat capacity is  $\rho c = 3.4533 \times 10^6 \text{ J/m}^3 \text{ }^\circ\text{C}$ , so the thermal diffusivity is  $\kappa = k/\rho c = 1.205 \times 10^{-7} \text{ m}^2/\text{s}$ . (For comparison, water is about  $1.4 \times 10^{-7} \text{ m}^2/\text{s}$ .) We will take the thickness of the food to be  $L = 10^{-2} \text{ m}$ . A hot plate is typically at about  $T_H = 200 \text{ }^\circ\text{C}$ , the ambient air temperature about  $T_C = 25 \text{ }^\circ\text{C}$ , so  $\Delta T = 175 \text{ }^\circ\text{C}$ . A good temperature for cooked beef is about  $T_{\text{cook}} = 70 \text{ }^\circ\text{C}$ .

Given all these dimensional parameters, we nondimensionalize the system by using  $L = 10^{-2} \text{ m}$  as a length scale. For a time scale we use the typical conductive time scale  $L^2/\kappa = 830 \text{ s}$  (almost 14 minutes). The temperature scale is  $\Delta T = T_H - T_C = 175 \text{ }^\circ\text{C}$ . Finally, we fix the energy scale to be  $k\Delta T L^3/\kappa = 604.3 \text{ J}$ . The physical parameters and their nondimensional versions are summarized in Table 1.

Table 1: Physical parameters used in the paper. When made dimensionless, temperatures are shifted by  $T_C$  before being scaled by  $\Delta T$ .

notation	value	d'less	description
$L$	0.01 m	1	food thickness (length scale)
$L^2/\kappa$	830 s	1	diffusive time (time scale)
$\Delta T$	175 $^\circ\text{C}$	1	temperature difference (temperature scale)
$T_H$	200 $^\circ\text{C}$	1	bottom temperature
$T_C$	25 $^\circ\text{C}$	0	top temperature (also initial temp.)
$T_{\text{cook}}$	70 $^\circ\text{C}$	0.257	cooked temperature
$h_0$	900 $\text{W/m}^2 \text{ }^\circ\text{C}$	21.6	bottom heat transfer coefficient
$h_1$	60 $\text{W/m}^2 \text{ }^\circ\text{C}$	1.44	top heat transfer coefficient
$\kappa$	$1.205 \times 10^{-7} \text{ m}^2/\text{s}$	1	thermal diffusivity of food
$k$	0.416 $\text{W/m}^\circ\text{C}$	1	thermal conductivity of food
$\rho c$	$3.4533 \times 10^6 \text{ J/m}^3 \text{ }^\circ\text{C}$	1	volumetric heat capacity of food
$\mu_1$		2.0803	first eigenvalue for Eq. (3.8)
$\mu_2$		4.7865	second eigenvalue
$\mu_3$		7.6966	third eigenvalue

We make the system dimensionless by letting  $z = \tilde{z}/L$ ,  $t = \kappa \tilde{t}/L^2$ , and  $T(z, t) = (\tilde{T}(\tilde{z}, \tilde{t}) - T_C)/\Delta T$  with  $\Delta T = T_H - T_C$ ; we then have the PDE system

$$T_t = T_{zz}, \quad 0 < z < 1, \quad t > 0, \quad (2.2a)$$

$$T(z, 0) = T_0(z), \quad 0 < z < 1, \quad (2.2b)$$

$$T_z(0, t) = -h_0 (1 - T(0, t)), \quad t > 0, \quad (2.2c)$$

$$T_z(1, t) = -h_1 T(1, t), \quad t > 0, \quad (2.2d)$$

where  $h_i = L \tilde{h}_i / k$ . In the remainder of the paper we use dimensionless quantities unless otherwise noted. We will typically take  $T_0(z) \equiv 0$ : the food starts at room temperature.<sup>2</sup>

### 3. Solving the heat equation

The solution of the system (2.2) is a standard exercise in linear PDEs [6]. We briefly outline the method here for completeness, and to fix the notation.

#### 3.1. The steady profile and temperature deviation

Let's solve the steady problem for Eq. (2.2) first, with the steady linear profile  $T(z, t) = S(z) = a + bz$ . After applying the boundary conditions (2.2c)–(2.2d), we find<sup>3</sup>

$$S(z) = \frac{h_0(1 + h_1 - h_1 z)}{h_0 + h_1 + h_0 h_1} = S(0) - \Delta S z, \quad \Delta S := S(0) - S(1), \quad (3.1)$$

<sup>2</sup>The MATLAB function `heat` solves Eq. (2.2) for a given initial condition.

<sup>3</sup>The MATLAB function `heatsteady` computes the steady temperature profile (3.1).

with

$$S(0) = \left(1 + \frac{h_1/h_0}{1+h_1}\right)^{-1} \leq 1, \quad S(1) = \left(1 + h_1 + \frac{h_1}{h_0}\right)^{-1} \leq 1. \quad (3.2)$$

For large  $h_0$  and small  $h_1$ , we have

$$S(0) \simeq 1 - h_1/h_0, \quad S(1) \simeq 1 - h_1, \quad (3.3)$$

so both the top and bottom temperatures are near 1, that is, the steady profile is nearly uniform. For  $h_0 = \infty$  and  $h_1 = 0$ , we have  $S(z) = 1$ .

We use Eq. (3.1) to reformulate (2.2) as a homogeneous problem for the temperature deviation

$$\theta(z, t) = T(z, t) - S(z), \quad (3.4)$$

which satisfies

$$\theta_t = \theta_{zz}, \quad 0 < z < 1, \quad t > 0, \quad (3.5a)$$

$$\theta(z, 0) = \theta_0(z) = T_0(z) - S(z), \quad 0 < z < 1, \quad (3.5b)$$

$$\theta_z(0, t) = h_0 \theta(0, t), \quad t > 0, \quad (3.5c)$$

$$\theta_z(1, t) = -h_1 \theta(1, t), \quad t > 0. \quad (3.5d)$$

The typical initial condition  $T_0(z) \equiv 0$  (room temperature) becomes  $\theta_0(z) = -S(z)$ . In Section 3.2 we show how to solve Eq. (3.5), and hence Eqs. (2.1) and (2.2), by an eigenfunction expansion.

### 3.2. Solution by eigenfunction expansion

The PDE system (3.5) is solved by separation of variables. Writing the separated solution  $\theta(z, t) = \phi(z)\tau(t)$ , we have

$$\frac{\tau_t}{\tau} = \frac{\phi_{zz}}{\phi} = -\mu^2 = \text{const.}, \quad (3.6)$$

where  $\mu^2 \in \mathbb{R}$  is the separation constant. For  $\mu = 0$ , we have  $\tau = \text{const.}$  and  $\phi(z) = A + Bz$ . The boundary conditions (3.5c)–(3.5d) lead to  $(h_0 + h_1 + h_0 h_1)A = 0$ , so we get the trivial solution; hence, we must have  $\mu \neq 0$ . It is straightforward to show that imaginary  $\mu$  can be ruled out by the boundary conditions as well [6].

Taking  $\mu > 0$  without loss of generality, we write the general separated solution to Eq. (3.6) as

$$\tau(t) = e^{-\mu^2 t}, \quad \phi(z) = A \cos \mu z + B \sin \mu z. \quad (3.7)$$

Applying the boundary conditions Eqs. (3.5c) and (3.5d) to  $\phi(z)$ , we obtain  $Ah_0 = \mu B$  and the transcendental equation

$$\frac{(h_0 + h_1)\mu}{\mu^2 - h_0 h_1} = \tan \mu, \quad \mu > 0. \quad (3.8)$$

In general the possible solutions  $\mu_m$ ,  $m = 1, 2, 3, \dots$ , have to be found numerically.<sup>4</sup> We order them such that  $\mu_1 < \mu_2 < \dots$ . Note that these are all distinct, being the eigenvalues of a Sturm–Liouville problem [6, p. 86]. For the parameters in Table 1, the first few roots are  $\mu_1 \approx 2.0803$ ,  $\mu_2 \approx 4.7865$ ,  $\mu_3 \approx 7.6966$ ,  $\mu_4 \approx 10.6709$ . The root  $\mu_m$  approaches a multiple of  $\pi$  for  $m$  large.

The L<sup>2</sup>-normalized eigenfunctions corresponding to the  $\mu_m$  can be written

$$\phi_m(z) = C_m^{-1} (\sin \mu_m z + (\mu_m/h_0) \cos \mu_m z), \quad m = 1, 2, 3, \dots \quad (3.9)$$

with the normalization constant  $C_m > 0$  defined as

$$C_m^2 = \frac{1}{2}(1 + (\mu_m/h_0)^2) + h_0^{-1} \sin^2 \mu_m + \frac{1}{4}(\mu_m h_0^{-2} - \mu_m^{-1}) \sin 2\mu_m. \quad (3.10)$$

---

<sup>4</sup>See MATLAB functions `heateigval` and `heateigfun`.

Because they are Sturm–Liouville eigenfunctions, the  $\phi_m$  satisfy orthogonality relations with respect to the standard  $L^2$  inner product:

$$\langle \phi_m, \phi_n \rangle = \delta_{mn}, \quad \langle f, g \rangle := \int_0^1 f(z) g(z) dz. \quad (3.11)$$

Now we expand the initial condition for  $\theta(z, t)$  in terms of these orthogonal eigenfunctions to obtain a generalized Fourier series<sup>5</sup>

$$\theta_0(z) = \sum_{m=1}^{\infty} \hat{\theta}_{0m} \phi_m(z), \quad (3.12)$$

where for any function  $f(z)$  the Fourier coefficients are

$$\hat{f}_m = \langle f, \phi_m \rangle. \quad (3.13)$$

Given this, the full solution to  $\theta(z, t)$  in (3.5) is immediate:

$$\theta(z, t) = \mathcal{H}_t \theta_0(z) = \sum_{m=1}^{\infty} \hat{\theta}_{0m} e^{-\mu_m^2 t} \phi_m(z). \quad (3.14)$$

Here we define the heat operator  $\mathcal{H}_t$  and heat kernel  $H$  as

$$\mathcal{H}_t \theta_0(z) = \int_0^1 H(z, t; z', 0) \theta_0(z') dz', \quad H(z, t; z', 0) = \sum_{m=1}^{\infty} e^{-\mu_m^2 t} \phi_m(z) \phi_m(z'). \quad (3.15)$$

We add the steady profile  $S(z)$  to (3.14) to obtain the solution to (2.2):

$$T(z, t) = S(z) + \mathcal{H}_t \theta_0(z) = S(z) + \sum_{m=1}^{\infty} \hat{\theta}_{0m} e^{-\mu_m^2 t} \phi_m(z). \quad (3.16)$$

We can expand  $S(z)$  itself in terms of the eigenfunctions:

$$S(z) = \sum_{m=1}^{\infty} \hat{S}_m \phi_m(z), \quad (3.17)$$

so our typical initial condition  $\theta_0(z) = -S(z)$  becomes  $\hat{\theta}_{0m} = -\hat{S}_m$  in terms of Fourier coefficients. Since the Fourier coefficients of the steady profile  $S(z)$  play an important role, we observe that we can compute them directly by integrating Eq. (3.1) against (3.9) to obtain

$$\hat{S}_m = (\mu_m C_m)^{-1} > 0 \quad (3.18)$$

where  $C_m$  is defined in Eq. (3.10).

#### 4. Cooking without flipping

Let's examine what happens if we just leave the food on the heating plate for a long time, without flipping. The Fourier coefficients of  $\theta(z, t)$  evolve according to Eq. (3.14),

$$\hat{\theta}_m(t) = -\hat{S}_m e^{-\mu_m^2 t} \quad (4.1)$$

where we took  $\hat{\theta}_{0m} = -\hat{S}_m$  (i.e.,  $T_0 \equiv 0$ ). For moderately large  $t$ , let's approximate the temperature at time  $t$  by keeping only the first eigenfunction:

$$T(z, t) \approx S(z) - \hat{S}_1 e^{-\mu_1^2 t} \phi_1(z). \quad (4.2)$$

---

<sup>5</sup>Generalized in the sense that the orthogonal functions are the  $\phi_m$ s, not the individual sines and cosines.

Now assume we have a dimensionless target cooking temperature  $T_{\text{cook}}$ , with  $0 < T_{\text{cook}} \leq S(0)$ , where  $S(0)$  is the hottest point of the steady solution. The criterion for the food to have cooked through to  $z = 1$  without needing to flip is

$$S(1) - \widehat{S}_1 e^{-\mu_1^2 t} \phi_1(1) = T_{\text{cook}}, \quad (4.3)$$

where  $S(1)$  is the coldest point of the steady solution. We can solve (4.3) for  $t$  to obtain the ‘cookthrough time’ for the food to cook without needing a flip:

$$t_{\text{cookthrough}} = \frac{1}{\mu_1^2} \log \left( \frac{\widehat{S}_1 \phi_1(1)}{S(1) - T_{\text{cook}}} \right), \quad e^{-(\mu_2^2 - \mu_1^2) t_{\text{cookthrough}}} \ll 1. \quad (4.4)$$

Here  $\widehat{S}_1 \phi_1(1) > 0$  for  $h_1 < \infty$ , and we need  $T_{\text{cook}} < S(1)$  for the cookthrough time to be well-defined. We conclude that for  $S(1) \leq T_{\text{cook}} \leq S(0)$ , flipping the food is required for cooking. In particular, for  $h_1 = \infty$  (perfect conductor at the top), we have  $\phi_1(1) = 0$ , and the top of the food remains at zero temperature no matter how long we wait.

However,  $t_{\text{cookthrough}}$  is typically rather large: for the parameters in Table 1, we have  $t_{\text{cookthrough}} \approx 0.340$ , or 283 s in dimensional terms.<sup>6</sup> This is not that long, since the food is fairly thin, but we will see that the cooking time can be greatly shortened by flipping, as of course experience suggests.

## 5. Flipping the food

In Section 3 we solved the PDE (2.2) and derived the time evolution of  $T(z, t)$  in terms of Fourier coefficients, as given by Eq. (3.16). We then found in Section 4 that it is sometimes possible to cook without flipping, as long as the steady top temperature  $S(1) > T_{\text{cook}}$ , though this can take a long time depending on the boundary conditions. In the present section we model a ‘flip’ of the food, that is, turning the food over on the hot plate.

### 5.1. Flipping at fixed intervals

There are two possible, mathematically-equivalent, approaches to deal with the ‘flipping’ of the food on the hot surface: flip the food (the  $[0, 1]$  domain itself), or flip the boundary conditions. In the context of solid and fluid mechanics, we can think of these as the Eulerian (fixed frame) and Lagrangian (moving frame) pictures, respectively. Here it is fairly easy to convert between both pictures, and we choose to flip the food (Eulerian). With this choice we have to ensure the  $z$  coordinate labels the same point in the food when determining if it is cooked. We will return to this issue in Section 7, when we look for optimal solutions.

Consider a slab with vertical temperature distribution  $T(z)$ ,  $0 < z < 1$ . If we flip the slab over, we obtain its new vertical temperature by replacing  $z$  by  $1 - z$ . We write this in terms of the ‘flipping operator’ defined by

$$\mathcal{F}f(z) = f(1 - z). \quad (5.1)$$

It is easy to see that this operator is self-adjoint with respect to the inner product (3.11). It has eigenvalues  $\pm 1$  and its eigenfunctions consist of even and odd functions with respect to  $z = 1/2$ .

Now define the ‘flip-and-heat’ operation, where we take an initial heat profile  $T(z, t)$ , flip it using (5.1), then allow it to evolve for a time  $\Delta t$ .<sup>7</sup> From Eq. (3.16), the temperature profile at time  $t + \Delta t$  is

$$T(z, t + \Delta t) = S(z) + \mathcal{H}_{\Delta t}(\mathcal{F}T(z, t) - S(z)). \quad (5.2)$$

We can solve this recurrence relation to obtain at time  $t_k = k\Delta t$

$$\begin{aligned} T(z, t_k) &= \mathcal{K}_{\Delta t}^k T_0(z) + \sum_{j=0}^{k-1} \mathcal{K}_{\Delta t}^j (1 - \mathcal{H}_{\Delta t}) S(z) \\ &= \mathcal{K}_{\Delta t}^k T_0(z) + (1 - \mathcal{K}_{\Delta t})^{-1} (1 - \mathcal{K}_{\Delta t}^k) (1 - \mathcal{H}_{\Delta t}) S(z) \end{aligned} \quad (5.3)$$

<sup>6</sup>See MATLAB function `tcookthru`; for our parameters, the approximate solution Eq. (4.4) is accurate to 0.07%.

<sup>7</sup>Since our initial condition  $T(z, 0) = 0$  is  $\mathcal{F}$ -invariant, it is immaterial whether we flip at the beginning or the end of the interval  $[t, t + \Delta t]$ .

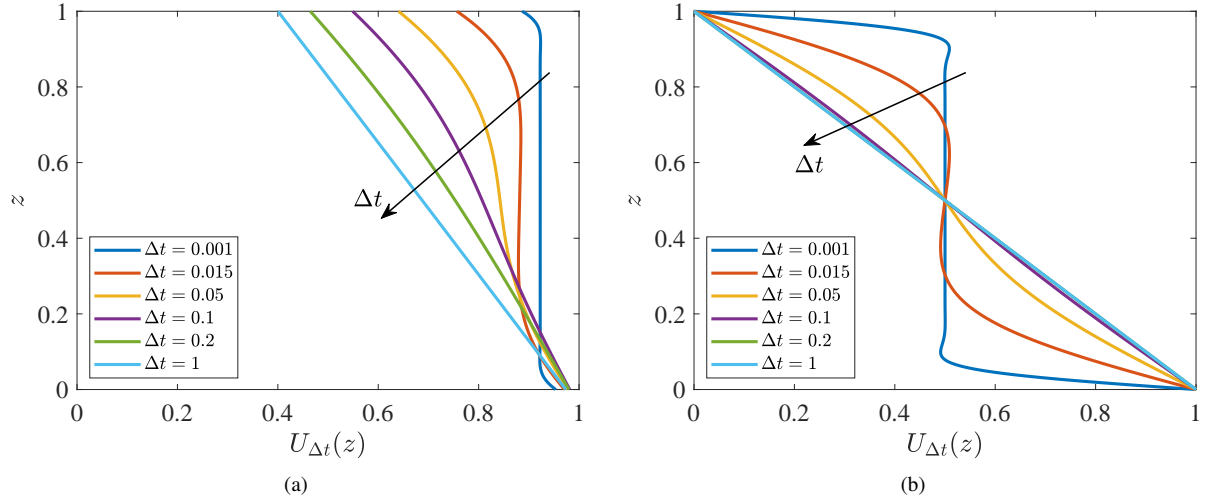


Figure 2: Asymptotic temperature profile  $U_{\Delta t}(z)$  for (a) the physical parameters from Table 1; (b) perfect conductors  $h_0 = h_1 = \infty$  at top and bottom. The better insulation at the top in (a) leads to much higher temperatures. In both cases, rapid flipping leads to a uniform asymptotic temperature  $\bar{U}$  in the interior, with boundary layers near the edges.

where the *flip-heat operator* is

$$\mathcal{K}_{\Delta t} := \mathcal{H}_{\Delta t} \mathcal{F}. \quad (5.4)$$

Since  $\|\mathcal{K}_{\Delta t}\| < 1$ ,  $T(z, t_k)$  converges to

$$U_{\Delta t}(z) := (1 - \mathcal{K}_{\Delta t})^{-1} (1 - \mathcal{H}_{\Delta t}) S(z) \quad (5.5)$$

as  $k \rightarrow \infty$ . This is the fixed point for the map (5.2). The rate of convergence is determined by the modulus of the eigenvalues of  $\mathcal{K}_{\Delta t}$ . Note that in a material (Lagrangian) frame moving with the food,  $U_{\Delta t}(z)$  is *not* a fixed point, but rather it flips at every interval.

Figure 2 shows numerical solutions for  $U_{\Delta t}(z)$  for several values of  $\Delta t$ , for the reference values in Table 1 (Fig. 2(a)) and for fixed temperature at both boundaries (Fig. 2(b),  $h_0 = h_1 = \infty$ ).<sup>8</sup> For large  $\Delta t$ ,  $U_{\Delta t}$  converges to the steady conduction profile  $S$ . For small  $\Delta t$ ,  $U_{\Delta t}$  limits to a constant temperature in the interior, with boundary layers at  $z = 0$  and  $1$ . The presence of the boundary layers can be attributed to the rapid flipping: the heat flux from the edges only penetrates a depth  $\sqrt{\Delta t}$  in the interior at each flip. This kind of profile is reminiscent of the mean temperature in turbulent Rayleigh–Bénard convection [2, Fig. 15]. The interior is ‘well-mixed,’ so the temperature is uniform, with boundary layers in order to satisfy the boundary conditions. The small overshoot seen in Fig. 2(b) is also present in convection, though the overshoot there tends to be larger. (In Appendix A we derive a precise expression for the boundary layer solution in Fig. 2(b) for the limit of small  $\Delta t$ .)

### 5.2. The internal temperature $\bar{U}$ for rapid flipping

The presence of boundary layers with a constant bulk temperature allows us to make a simple argument to predict the form of  $U_{\Delta t}$  as  $\Delta t \rightarrow 0$ , that is, when the flips are short. Figure 3 shows schematically what the limiting profile looks like, with a bulk temperature  $\bar{U}$  and boundary layers of thickness  $\Delta z$ . Since  $U_{\Delta t}$  must satisfy Eqs. (2.2c) and (2.2d), we have

$$\frac{\bar{U} - U_0}{\Delta z_0} \approx -h_0 (1 - U_0), \quad \frac{U_1 - \bar{U}}{\Delta z_1} \approx -h_1 U_1, \quad (5.6)$$

<sup>8</sup>See MATLAB function `flipheatfix`.

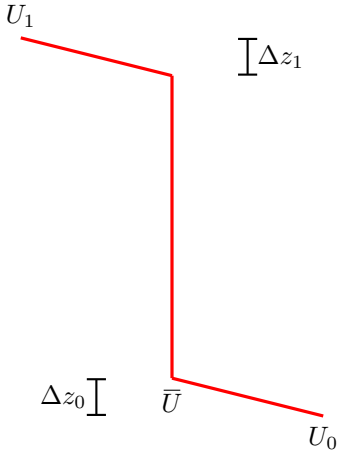


Figure 3: Schematic representation of  $U_{\Delta t}(z)$  for small  $\Delta t$ . The temperature at  $z = 0, 1$  is  $U_{0,1}$ ,  $\bar{U}$  is the temperature in the bulk, and the boundary layers are of thickness  $\Delta z_{0,1}$ .

where we approximated derivatives by the slope in the boundary layers in Fig. 3. We want the limit  $\Delta z_i \rightarrow 0$  to exist, so we demand

$$\bar{U} - U_0 = O(\Delta z_0) \quad U_1 - \bar{U} = O(\Delta z_1), \quad \Delta z_i \rightarrow 0. \quad (5.7)$$

Subtracting these, we have

$$\bar{U} = \frac{1}{2}(U_0 + U_1) + O(\Delta z_i). \quad (5.8)$$

We can also write this as

$$U_0 = \bar{U} + \Delta U, \quad U_1 = \bar{U} - \Delta U. \quad (5.9)$$

Returning to Eq. (5.6), we have

$$-\frac{\Delta U}{\Delta z_0} \approx -h_0(1 - U_0), \quad -\frac{\Delta U}{\Delta z_1} \approx -h_1 U_1. \quad (5.10)$$

The fluxes  $\Delta U/\Delta z_i$  in Eq. (5.10) must be equal, since otherwise the fixed-point profile would have a net gain or loss of heat during an interval  $\Delta t$ . This means that  $\Delta z_0 = \Delta z_1$  (the boundary layers have the same thickness), and we can equate the two right-hand sides in Eq. (5.10) to obtain

$$\bar{U} \approx \frac{h_0}{h_0 + h_1}, \quad \Delta t \rightarrow 0. \quad (5.11)$$

For the parameters in Table 1, this gives  $\bar{U} \approx 0.9375$ , in good agreement with the small- $\Delta t$  case in Fig. 2(a). For symmetric cases with  $h_0 = h_1$ , we always have  $\bar{U} = 1/2$ , as is apparent in Fig. 2(b). Note that to maximize  $\bar{U}$  in Eq. (5.11) we should make  $h_1$  as small as possible for a given  $h_0$ , that is, make the top boundary as insulating as possible. For  $h_1 = 0$  (perfect insulator) we have  $\bar{U} = 1$ , independent of  $h_0$ .

### 5.3. Eigenfunction formulation

The projection of the flipped eigenfunctions onto the upright (unflipped) eigenfunctions is

$$F_{mn} = \langle \mathcal{F}\phi_m, \phi_n \rangle = \int_0^1 \mathcal{F}\phi_m(z) \phi_n(z) dz. \quad (5.12)$$

The matrix  $F$  is symmetric, as can be seen by putting  $\tilde{z} = 1 - z$  in Eq. (5.12):

$$F_{mn} = \int_0^1 \phi_m(1 - z) \phi_n(z) dz = \int_0^1 \phi_m(z') \phi_n(1 - z') dz' = F_{nm}.$$

The Fourier matrix representation of the flip-heat operator  $\mathcal{K}_{\Delta t}$  from (5.4) is

$$(\mathcal{K}_{\Delta t})_{mn} = \langle \mathcal{K}_{\Delta t} \phi_m, \phi_n \rangle = e^{-\mu_m^2 \Delta t} F_{mn}. \quad (5.13)$$

Its transpose is the heat-flip operator, where we heat first for a time  $\Delta t$  and then flip.

The Fourier representation of Eq. (5.3) with  $T_0(z) = 0$  is

$$\widehat{T}_m(t_k) = \sum_{n=1}^{\infty} [(I - K_{\Delta t})^{-1} (I - K_{\Delta t}^k)]_{mn} (1 - e^{-\mu_n^2 \Delta t}) \widehat{S}_n, \quad (5.14)$$

which for large  $k$  converges to the fixed-point profile

$$(\widehat{U}_{\Delta t})_m = \sum_{n=1}^{\infty} [(I - K_{\Delta t})^{-1}]_{mn} (1 - e^{-\mu_n^2 \Delta t}) \widehat{S}_n. \quad (5.15)$$

Though these expressions are computationally useful, they are difficult to use for analytical progress, except in the symmetric case that we treat in Section 6.

#### 5.4. The spectrum of $\mathcal{K}_{\Delta t}$

As mentioned in Section 5.1, the rate of convergence of temperature to the fixed-point profile  $U_{\Delta t}$  is determined by the spectrum of the flip-heat operator  $\mathcal{K}_{\Delta t} = \mathcal{H}_{\Delta t} \mathcal{F}$ . Write  $\psi_m(z)$  and  $\sigma_m$  for the eigenfunctions and eigenvalues of  $\mathcal{K}_{\Delta t}$ :

$$\mathcal{K}_{\Delta t} \psi_m(z) = \sigma_m \psi_m(z). \quad (5.16)$$

(We suppress the  $\Delta t$  dependence of  $\psi_m$  and  $\sigma_m$  to keep the notation light.) Let  $\chi_m(z) = \mathcal{F} \psi_m(z)$  be the ‘flipped’ eigenfunction:

$$\mathcal{K}_{\Delta t} \psi_m(z) = \mathcal{H}_{\Delta t} \chi_m(z) = \sigma_m \mathcal{F} \chi_m(z). \quad (5.17)$$

Multiplying by  $\chi_n(z)$  and integrating, we have

$$\langle \chi_n, \mathcal{H}_{\Delta t} \chi_m \rangle = \sigma_m \langle \chi_n, \mathcal{F} \chi_m \rangle. \quad (5.18)$$

Because both  $\mathcal{H}_{\Delta t}$  and  $\mathcal{F}$  are self-adjoint, we can interchange  $m$  and  $n$  to get

$$(\sigma_m - \sigma_n) \langle \chi_n, \mathcal{F} \chi_m \rangle = 0. \quad (5.19)$$

Hence, the eigenfunctions  $\psi_m(z)$  are  $\mathcal{F}$ -orthogonal:

$$\langle \psi_m, \mathcal{F} \psi_n \rangle = 0, \quad \sigma_m \neq \sigma_n. \quad (5.20)$$

The self-adjointness of  $\mathcal{H}_{\Delta t}$  and  $\mathcal{F}$  also implies that the  $\sigma_m$  are real. Note that, unlike the eigenvalues of  $\mathcal{H}_{\Delta t}$ , here eigenvalues alternate sign:  $\sigma_m = (-1)^{m+1} |\sigma_m|$ .

Recall that the eigenvalues of the heat operator  $\mathcal{H}_{\Delta t}$  are  $e^{-\mu_m^2 \Delta t}$ . In order to compare decay rates with and without flipping, we define the decay rate  $\nu_m > 0$  by

$$\nu_m^2 = -\frac{1}{\Delta t} \log |\sigma_m|, \quad m = 1, 2, 3, \dots \quad (5.21)$$

The  $\nu_m$  can be compared to the  $\mu_m$  to quantify how flipping accelerates convergence to the fixed-point profile  $U_{\Delta t}$ , versus convergence to the steady solution  $S(z)$  in the absence of flipping. Unlike  $\mu_m$ ,  $\nu_m$  depends on the flip interval  $\Delta t$ . For large  $\Delta t$  the  $\nu_m$  converge to the  $\mu_m$ . For small  $\Delta t$ , the limit is nontrivial: in Fig. 4 we can see that  $\nu_1$  converges to approximately 2.685 as  $\Delta t \rightarrow 0$ , for the reference parameter values in Table 1. This is significantly faster than the corresponding unflipped eigenvalue  $\mu_1 \approx 2.0803$  for the same parameter values. The acceleration ratio is thus

$$\frac{\nu_1^2}{\mu_1^2} \approx \frac{(2.685)^2}{(2.0803)^2} \approx 1.67, \quad \Delta t \rightarrow 0, \quad (5.22)$$

that is, in the limit of very rapid flips, the approach to equilibrium is about 2/3 faster. This does not mean that the total cooking time is that much faster, since it also depends on the profile  $U_{\Delta t}$ . As we will see in Section 6, for the symmetric case  $h_0 = h_1$  we have  $\nu_1 = \mu_1$ , and yet the cooking time is still much faster with flipping than without. A rigorous proof of the existence of the limit (5.22), or an estimate of its value, is an interesting open question.

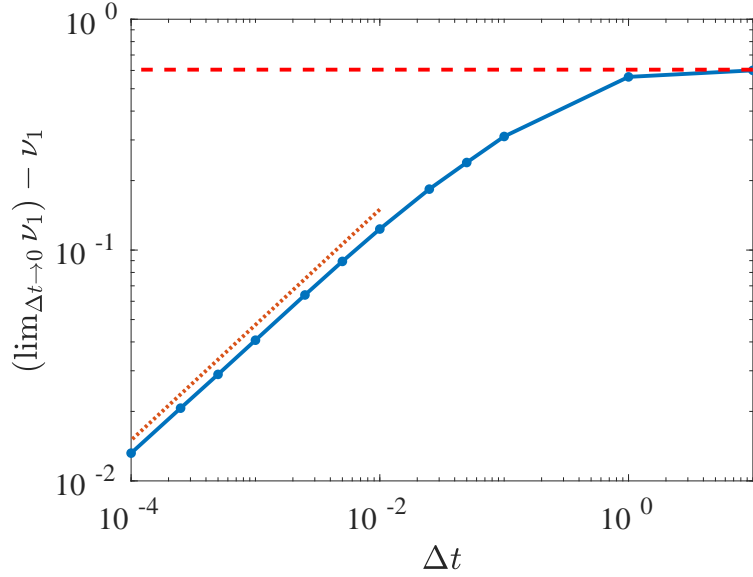


Figure 4: Dependence on  $\Delta t$  of the leading decay rate  $\nu_1$  [Eq. (5.21)] for the flip-heat operator  $\mathcal{K}_{\Delta t}$ . The limit of  $\nu_1$  as  $\Delta t \rightarrow 0$  is about 2.685, with convergence at a rate  $\sqrt{\Delta t}$  (dotted line). The horizontal dashed line indicates  $\mu_1$  for the heat operator.

## 6. Symmetric case ( $h_0 = h_1$ )

Things simplify considerably for the up-down symmetric case  $h_0 = h_1$ . The system as a whole is still asymmetric in that it is heated at  $z = 0$  and cooled at  $z = 1$ , but the material properties are the same on the top and bottom. This could be achieved by placing on top of the food an unheated metal plate with the same properties as the bottom heating plate. For instance, a top metal plate is used to make thin ‘smashed burgers.’ The symmetric case is analogous to the Boussinesq limit for Rayleigh–Bénard convection, as opposed to the non-Boussinesq case which has non-symmetric boundary conditions [10].

For this symmetric case, the flip and heat operators commute:

$$\mathcal{F}\mathcal{H}_t = \mathcal{H}_t\mathcal{F}. \quad (6.1)$$

The eigenfunctions  $\phi_m(z)$  of  $\mathcal{H}_t$  have the parity property

$$\mathcal{F}\phi_m(z) = (-1)^{m+1}\phi_m(z). \quad (6.2)$$

Hence, from Eq. (5.12),

$$F_{mn} = (-1)^{m+1} \delta_{mn}. \quad (6.3)$$

The eigenvalues and eigenfunctions of  $\mathcal{K}_t = \mathcal{H}_t\mathcal{F}$  are then

$$\sigma_m = (-1)^{m+1} e^{-\mu_m^2 t}, \quad \psi_m(z) = (-1)^{m+1} \phi_m(z), \quad (6.4)$$

and  $\nu_m = \mu_m$  in Eq. (5.21). Therefore, the *rate* of convergence to the fixed-point profile is not accelerated. The improvement in cooking time will arise because with flipping we expect that the final point to be cooked is close to  $z = 1/2$ , as opposed to  $z = 1$  without flipping (Section 4).

The steady-state profile (3.1) can be divided into a constant part (even under  $\mathcal{F}$ ) and a part proportional to  $z - \frac{1}{2}$  (odd under  $\mathcal{F}$ ):

$$\begin{aligned} S(z) &= \frac{1}{2}(S(0) + S(1)) - (S(0) - S(1))(z - \frac{1}{2}) \\ &= \frac{1}{2} - (1 + 2h_0^{-1})^{-1} (z - \frac{1}{2}). \end{aligned} \quad (6.5)$$

From Eq. (5.15), we have for the fixed-point profile

$$\begin{aligned} U_{\Delta t}(z) &= \sum_{m=1}^{\infty} \frac{1 - e^{-\mu_m^2 \Delta t}}{1 + (-1)^m e^{-\mu_m^2 \Delta t}} \widehat{S}_m \phi_m(z) \\ &= \sum_{m \text{ odd}} \widehat{S}_m \phi_m(z) + \sum_{m \text{ even}} \tanh(\mu_m^2 \Delta t/2) \widehat{S}_m \phi_m(z). \end{aligned} \quad (6.6)$$

The first sum is equal to the even (constant) part of the temperature profile (6.5), so (6.6) simplifies to:

$$U_{\Delta t}(z) = \frac{1}{2} + \sum_{m \text{ even}} \tanh(\mu_m^2 \Delta t/2) \widehat{S}_m \phi_m(z). \quad (6.7)$$

We then have  $U_{\Delta t}(\frac{1}{2}) = \frac{1}{2}$ , since  $\phi_m(\frac{1}{2}) = 0$  for  $m$  even. This is the type of fixed-point profile plotted in Fig. 2(b) for  $h_0 = h_1 = \infty$ . In Appendix A we determine the boundary layer structure from Eq. (6.7) in the limit of small  $\Delta t$ .

Because  $\mathcal{F}$  and  $\mathcal{H}_{\Delta t}$  commute, the recurrence solution to the flip-heat map (5.3) after  $k$  flips is

$$T(z, k\Delta t) = U_{\Delta t}(z) - \sum_m (-1)^{k(m+1)} e^{-\mu_m^2 k\Delta t} (\widehat{U}_{\Delta t})_m \phi_m(z), \quad (6.8)$$

where we take  $T(z, 0) = 0$  (food initially uniformly cold). Intuition suggests that the hardest point to cook is the center  $z = 1/2$ ; assuming that this is so (we will discuss this assumption below), the cooking time is obtained by solving

$$T_{\text{cook}} = T\left(\frac{1}{2}, t_{\text{cook}}\right) = \frac{1}{2} - \sum_{m \text{ odd}} e^{-\mu_m^2 t_{\text{cook}}} \widehat{S}_m \phi_m\left(\frac{1}{2}\right) \quad (6.9)$$

for  $t_{\text{cook}} = k\Delta t$ . This cannot be solved analytically, but let us see about finding  $t_{\text{cook}}$  by retaining only the slowest-decaying mode  $m = 1$ :

$$t_{\text{cook}} \approx \frac{1}{\mu_1^2} \log\left(\frac{\widehat{S}_1 \phi_1\left(\frac{1}{2}\right)}{\frac{1}{2} - T_{\text{cook}}}\right), \quad e^{-(\mu_3^2 - \mu_1^2) t_{\text{cook}}} \ll 1. \quad (6.10)$$

Compare with Eq. (4.4) for the cookthrough time.

Even though the cooking time  $t_{\text{cook}}$  is fairly short, the approximation (6.10) is remarkably accurate because the error depends on the ratio between  $e^{-\mu_3^2 t_{\text{cook}}}$  and  $e^{-\mu_1^2 t_{\text{cook}}}$ : eigenmodes that are odd under  $\mathcal{F}$  do not contribute to the temperature at the midpoint. For  $h_0 = h_1 = \infty$ , Eq. (6.10) gives

$$t_{\text{cook}} \approx \frac{1}{\pi^2} \log\left(\frac{2/\pi}{\frac{1}{2} - T_{\text{cook}}}\right) \approx 0.097568, \quad (6.11)$$

whereas solving Eq. (6.9) numerically gives  $t_{\text{cook}} \approx 0.097584$ .<sup>9</sup> What is striking about Eq. (6.10) is that it does not depend on the number of flips,  $k - 1$ , but only on the total time  $k\Delta t$ . This is clearly due to the commutativity of  $\mathcal{H}_{\Delta t}$  and  $\mathcal{F}$ .

Can this be true? It seems counter-intuitive that the cooking time is completely independent of how we choose to flip, as long as we flip at least once. Yet numerical simulations support this, with an important caveat. In Fig. 5(a) we show the ‘cooked fraction’ (defined more precisely in Section 7) as a function of time, for varying numbers of flips. These solutions all manage to cook the food in a time of 0.0976! And yet in Fig. 5(b) we show a different set of flips, and two cases take longer to cook. The explanation is likely that formula (6.11) assumes that the last point to be cooked is  $z = 1/2$ , whereas for these two simulations this point is quite far from  $z = 1/2$ .

---

<sup>9</sup>See MATLAB program `tcooksym`.

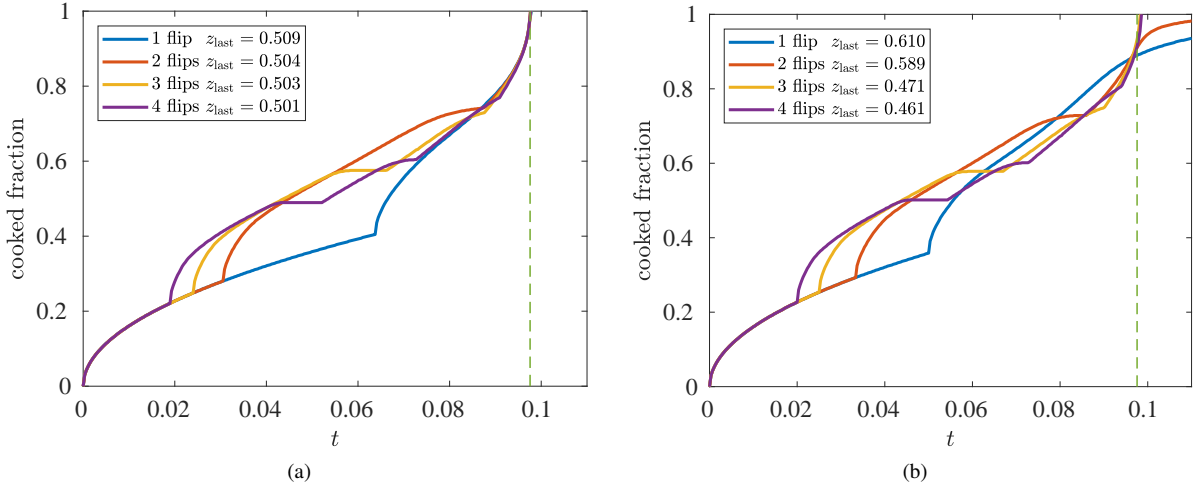


Figure 5: For symmetric perfectly-conducting boundary conditions  $h_0 = h_1 = \infty$ : (a) Cooked fraction as a function of time for optimal solutions for 1 to 4 flips. All the optimal times are essentially the same (0.0976), independent of the number of flips, and the final point to be cooked is always  $z \approx 0.5$ . (b) Cooked fraction for equal-time flips  $\Delta t = 0.1/k$ , where  $k = 1$  is the number of flips. The vertical dashed line is the numerically-obtained optimal cooking time 0.0976.

## 7. Optimizing the flipping times

In the previous sections we used the Eulerian description, where the food is flipped and the coordinate  $z$  refers to a fixed point in space. The Lagrangian or ‘co-flipping’ description is in terms of a material point  $z_0 \in [0, 1]$ , which corresponds to a fixed point inside the food. We can convert between the two pictures easily using the flip operator Eq. (5.1):

$$z = (\mathcal{F})^{\# \text{flips}(t)} z_0, \quad (7.1)$$

where  $\# \text{flips}(t)$  gives the number of flips until time  $t$ . Thus the two reference frames coincide until the first flip, after which  $z_0 = 1 - z$  until the next flip, etc.

In this section we will seek to optimize the time intervals where flips occur, in order to find the optimal cooking time. For this the Lagrangian description is the appropriate one, since we must keep track of the history of each material point in the food. With a small abuse of notation we will denote the temperature at material point  $z_0$  at time  $t$  by  $T_0(z_0, t)$ . (Recall that  $T_0(z)$  was the initial temperature profile.)

Note that in Section 6 we estimated a cooking time by finding when the center point  $z = 1/2$  was cooked. Since this point is the same in the Eulerian or Lagrangian frames, we did not have to change frames.

### 7.1. Cooking time for variable intervals

Recall that we declare the food to be cooked if every point  $z \in [0, 1]$  has at some time in its history achieved the temperature  $T_{\text{cook}}$ . We define the cooked fraction at time  $t$  as

$$\text{cooked fraction}(t) = \int_0^1 \left[ \max_{s \in [0, t]} T_0(z_0, s) \geq T_{\text{cook}} \right] dz_0 \quad (7.2)$$

where  $\llbracket A \rrbracket$  is the indicator function of  $A$ : it is one if  $A$  is true, and zero otherwise. The cooked fraction is a nondecreasing function of time, since points cannot ‘uncook.’ The cooking time is then

$$t_{\text{cook}} = \inf_{t \geq 0} \{ \text{cooked fraction}(t) = 1 \}. \quad (7.3)$$

The cooking time could be infinite, as we saw in Section 4 when cooking without flipping.

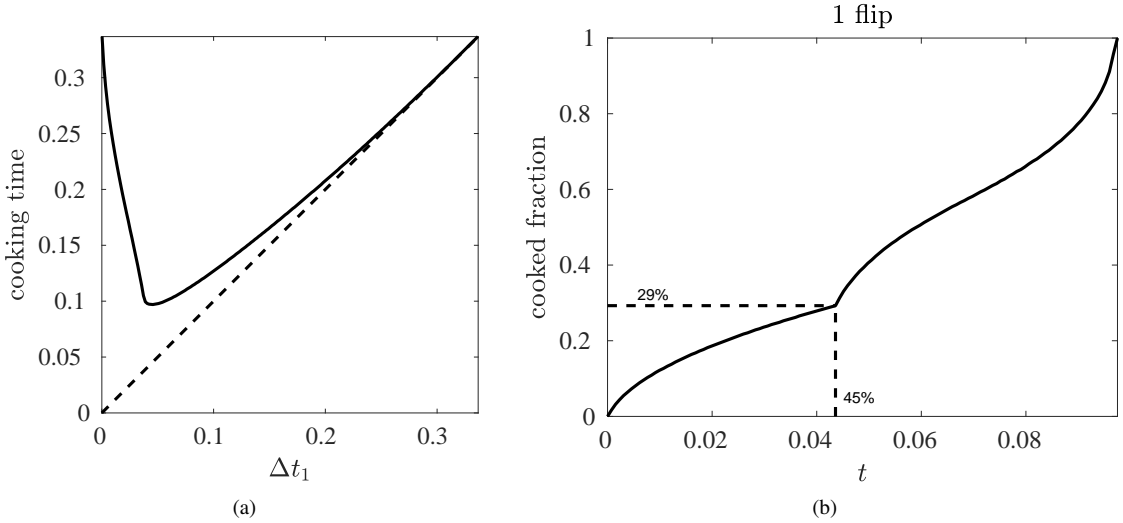


Figure 6: Cooking with one flip. (a) The total cooking  $t_{\text{cook}}$  time as a function of the flipping time  $\Delta t_1$ , showing a single minimum. The dashed line is the diagonal  $t_{\text{cook}} = \Delta t_1$ ; the solid curve crosses the dashed line at  $\Delta t_1 = t_{\text{cookthrough}} \approx 0.340$  (Section 4). (b) Cooked fraction as a function of time for the optimal solution (the minimum in (a)). The phase after the flip is longer, and there is rapid cooking at the very end. The percentages indicate that the food is 29% cooked at the optimal flipping time  $\Delta t_1 \approx 0.04359$ , which occurs at 45% of  $t_{\text{cook}}$ .

We specify a cooking protocol by fixing the number of cooking intervals  $k \geq 1$  as well as the flipping times

$$\Delta t_1, \Delta t_2, \dots, \Delta t_{k-1}, \quad \Delta t_j > 0. \quad (7.4)$$

Note that we do not allow any zero  $\Delta t_j$ , as this would effectively reduce to a cooking protocol with fewer flips. We define the length of the final cooking interval as

$$\Delta t_k = t_{\text{cook}} - \sum_{j=1}^{k-1} \Delta t_j > 0. \quad (7.5)$$

Figure 6(a) shows the cooking time  $t_{\text{cook}}$  as a function of  $\Delta t_1$ , for  $k = 2$  cooking intervals (1 flip).<sup>10</sup> The dashed line is the diagonal  $t_{\text{cook}} = \Delta t_1$ ; since  $t_{\text{cook}} = \Delta t_1 + \Delta t_2$  with  $\Delta t_2 > 0$ , the solid cooking time curve must lie above this diagonal. The curve for  $t_{\text{cook}}$  intersects the diagonal as  $\Delta t_1 \rightarrow t_{\text{cookthrough}}$ , since for these parameters the cookthrough time is not infinite; otherwise  $t_{\text{cook}}$  asymptotes to the diagonal. The cooking time  $t_{\text{cook}}$  also asymptotes to  $t_{\text{cookthrough}}$  as  $\Delta t_1 \rightarrow 0$ . Figure 6(a) suggests that there is a unique minimum cooking time for one flip,  $t_{\text{cook}} \approx 0.09751$ .

The shape of  $t_{\text{cook}}$  near the minimum in Fig. 6(a) has an important consequence: notice that  $t_{\text{cook}}$  is quite a bit steeper to the left of the minimum than to the right. This means that it is preferable to err to the *right* of the minimum (*i.e.*, waiting a bit longer to flip), since this does not increase the cooking time substantially. Making  $\Delta t_1$  too small, however, will necessitate a longer final phase of cooking.

Figure 7(a) shows the cooking time  $t_{\text{cook}}$  if we flip the food twice, with three time intervals  $[0, \Delta t_1]$ ,  $[\Delta t_1, \Delta t_1 + \Delta t_2]$ , and  $[\Delta t_1 + \Delta t_2, t_{\text{cook}}]$ . In the same manner as we saw for one flip, the figure suggests a unique global minimum. In the regions without data the food is cooked before the second flip occurs, so we ignore those values (*i.e.*, we plot nothing). As for the single-flip case, the steepness of the minimum suggests that we should cook slightly longer than the optimal values, since an error on the left has larger consequences.

<sup>10</sup>See MATLAB program `cooktime`.

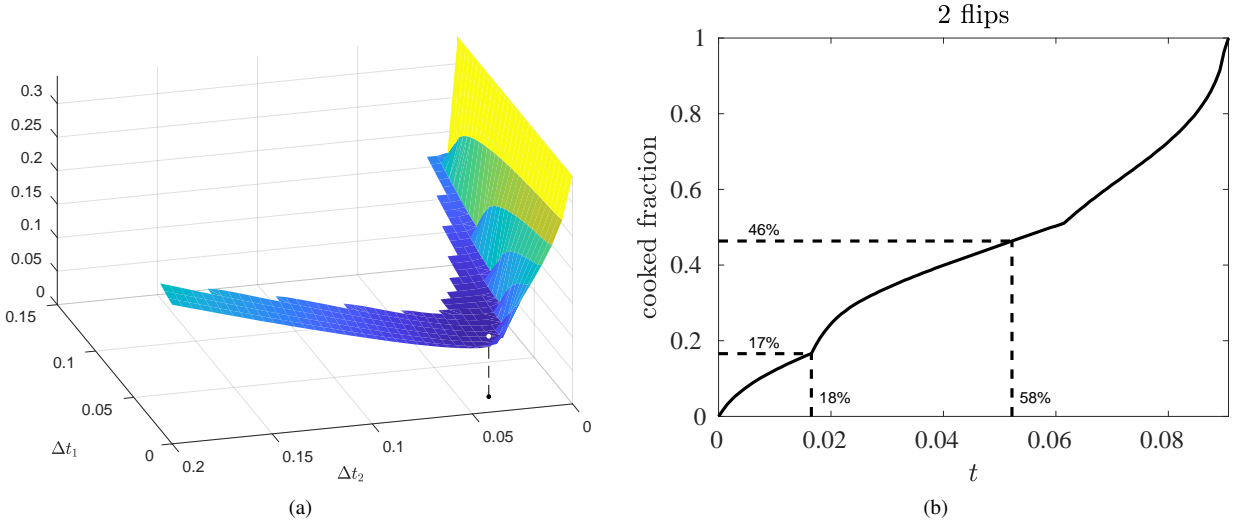


Figure 7: Cooking with two flips. (a) The total cooking time as a function of the length the two flipping intervals  $\Delta t_1$  and  $\Delta t_2$ , again showing a well-defined unique minimum. In the region without data the food is cooked before a second flip, so the region does not count as two flips. (b) Cooked fraction as a function of time for the optimal 2-flip solution. There is an 8% improvement in cooking time over a single flip. The time  $\Delta t_1$  is quite short, making up only 18% of the total cooking time. Note that the times with discontinuous slopes are not necessarily the flipping times.

## 7.2. Numerical optimization

Because of the nonlocal-in-time nature of the objective function (7.3), optimizing for the flipping times is difficult and necessitates a numerical approach. Furthermore, this optimization problem is likely nonconvex and we have no guarantees that we have found the global minimum. Despite this, the swift convergence and robustness of the code suggests that the minima we find are most likely global.

We use MATLAB's nonlinear optimization function `fminsearch` to look for combinations of cooking intervals that lead to the fastest total cooking time.<sup>11</sup> The optimal solution for 1 flip ( $k = 2$  two cooking intervals) is plotted in Fig. 6(b). We show the cooked fraction as a function of time, so we can see how much each cooking interval contributes to the total cooking. The first interval is somewhat shorter than the second, and it leads to far less cooking: the first interval is 45% of the total time, but leads only to 29% of the cooking. There is also a sudden spurt of cooking at the end of the second interval. This feature is present in optimal solutions with more flips as well, and suggests that an optimal solution seeks to build up a large temperature gradient that then diffuses and cooks rapidly.

The optimal solution for 2 flips ( $k = 3$  two cooking intervals) is plotted in Fig. 7(b). Again the first interval is relatively short, and does not lead to much cooking. The final interval is long (42% of total time), and gives a whopping 54% of the cooking. Observe that the curve has a point of discontinuous slope that doesn't coincide with a flip. This can be traced to the max function in our definition of the cooked fraction (7.2): when we flip the food, points that were on the top surface have cooled down, but have not uncooked. Some time is needed for the heat to propagate into the interior from the hot plate to resume cooking.

In Fig. 8 we increase the number of flips gradually. We observe that the cooking intervals become more evenly spaced, except for the final one. We push this to the limit in Fig. 9(a): there we show the optimal solution for 20 flips, which no chef should attempt. The intervals are very similar in length, except again for the final one. The improvement in optimal cooking time as a function of the number of flips, shown in Fig. 9(b), is fairly marginal after a few flips. The optimal cooking time appears to asymptote to a nonzero value.

To help visualize the cooking process, we show in Fig. 10 the cooked region in gray as a function of time for several optimal solutions. The top frame is the cooked region without flipping, which will cook at time  $t_{\text{cookthrough}} \approx 0.340$  (Section 4). The vertical is the Lagrangian coordinate  $z_0 \in [0, 1]$ . In that figure we are “co-flipping” with the food, *i.e.*, we are following material points.

<sup>11</sup>See MATLAB program `mincooktime`.

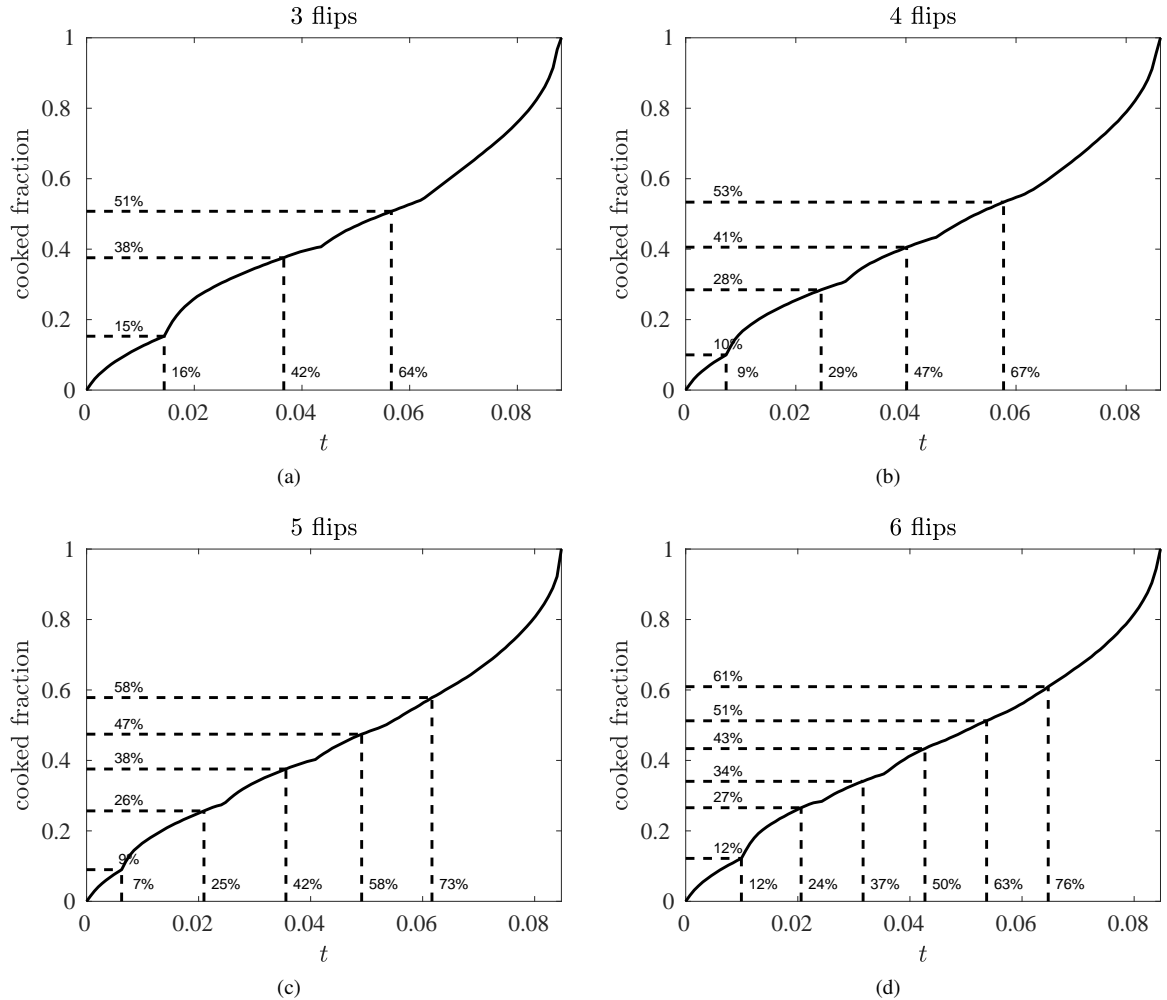


Figure 8: (a)–(d) Optimal flipping times for 3–6 flips. In each case the initial time  $\Delta t_1$  is fairly short, and the last interval is much longer. The improvement with more flips is marginal (see Fig. 9(b)).

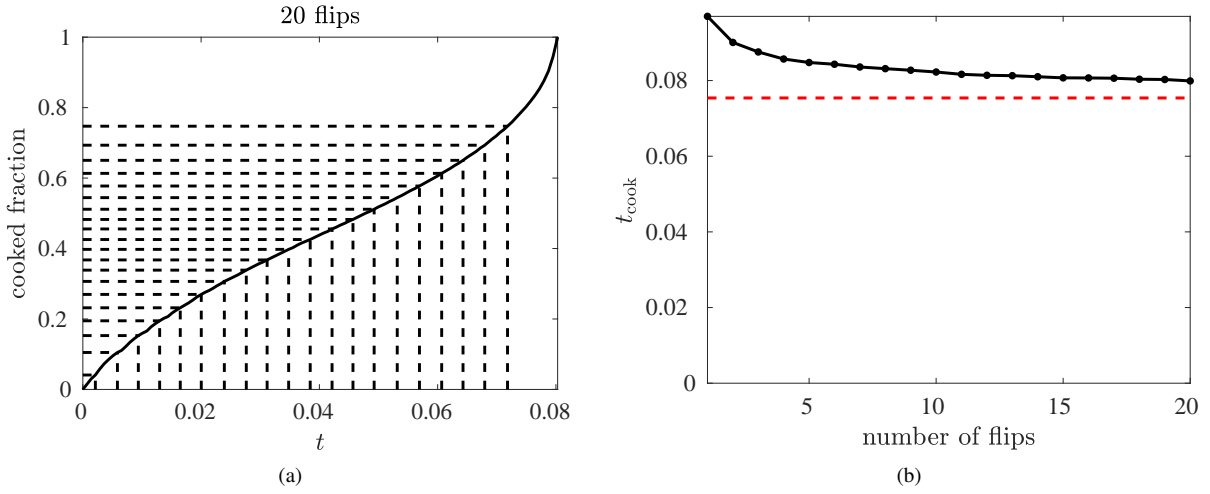


Figure 9: (a) The optimal times for 20 flips: the intervals now have very comparable lengths, except the final one which is about twice as long. (b) For a large number of flips, the optimal cooking time  $t_{\text{cook}}$  converges to  $\approx 0.0754$  (63 s), as compared to 0.0970 (80.5 s) for a single flip. This is a theoretical maximum decrease of 29% (close to the Food Lab prediction [3], see Section 1).

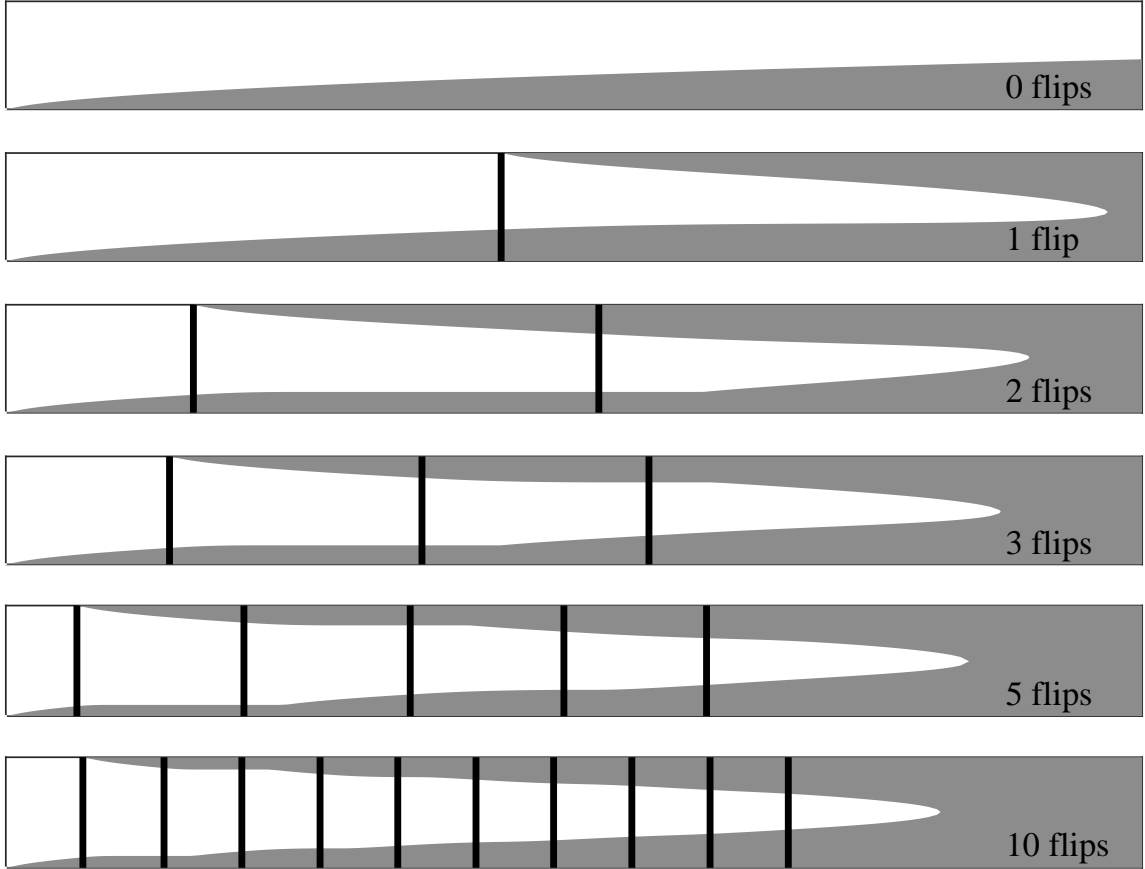


Figure 10: Comparison of optimal solutions for different number of flips. The vertical axis is the Lagrangian coordinate  $z_0 \in [0, 1]$ , and the cooked region is shown in gray as a function of time. The vertical lines indicate times of flipping. We can clearly see that the surface initially at the top does not begin cooking until the first flip. The time interval depicted (horizontal axis) is  $t \in [0, 0.1]$ . (Parameters as in Table 1.)

## 8. Discussion

In this paper we examined a simple model of cooking and flipping. We solved a one-dimensional heat equation with general boundary conditions in the form of Newton's law of cooling. We expressed the solution as a generalized Fourier series in Sturm–Liouville eigenfunctions. We saw immediately that the food might never fully reach its cooked temperature, unless it is flipped.

Flipping the food (*i.e.*, turning it over on the hot surface) can be regarded as applying a map  $z \mapsto 1 - z$  to the temperature field. Composing such an instantaneous flip with an interval  $\Delta t$  of heating gives the flip-heat operator. The spectral properties of this operator are themselves of some interest, but have only been scratched here. Of more importance than the spectrum for the purpose of cooking is the fixed point of this operator, which represents the equilibrium temperature after many flips. It is the increase in the interior temperature for this fixed point that is mostly responsible for the improved cooking (see Eq. (5.11) for small  $\Delta t$ ). A related idea arises in the mixing of fluid: in the presence of sources and sinks, it is often more practical to modify the target temperature distribution rather than the rate of approach to that target [8, 9].

The symmetric case, where the thermal properties at the top and bottom are the same, is most readily solvable. It exhibits some peculiarities, such as the independence on the duration of flipping intervals, as long as we flip at least once, and the final point to be cooked is the midpoint. This is only determined *a posteriori*, so it is an open question if a more practical criterion can be found. Note that the symmetric versus non-symmetric cases are the analogues of the Boussinesq versus non-Boussinesq cases in Rayleigh–Bénard convection [10].

Finally, we carried out numerical optimization of the cooking intervals. We fixed the number of flips, and found the flipping times that lead to the shortest total cooking time. The criterion for cooking is that all the points in the food exceed a certain temperature at some point in their history. Surprisingly, the numerical optimization appears to converge to a unique global minimum, though it is not obvious why this problem should behave like a convex one. For several flips, the optimal intervals of cooking are roughly of the same length, except for the final interval, which is typically longer and where much of the cooking actually occurs. The shape of the cooking time function for two and three flips suggests that it is better to err on the side of cooking a bit longer for each flip, since a shorter interval leads to a longer cooking time (that is, for two flips the derivative is much steeper to the left of the minimum than to the right; see Fig. 6(a)).

We emphasize that our results are mostly qualitative. In particular, they are too short by roughly a factor of two from typical cooking times. But the 29% decrease in total cooking time is relatively close to the Food Lab prediction [3] mentioned in our introduction. A realistic model of cooking should include many subtle effects, such as the change in moisture content and the melting of fat [1, 4, 5]. Of course, any partially analytic treatment as given here quickly becomes impossible as more effects are included.

## Acknowledgments

This project was originally inspired by Persi Diaconis and Susan Holmes. The author thanks Charles Doering for helpful discussions.

## References

- [1] M. Dagerskog. Time-temperature relationship in industrial cooking and frying. In T. Høyem and O. Kvåle, editors, *Physical, chemical and biological changes in foods caused by thermal processing*, pages 77–100. Applied Science Publishers, London, 1977. ISBN 9780853347293.
- [2] U. Hansen, D. A. Yuen, and A. V. Malevsky. Comparison of steady-state and strongly chaotic thermal convection at high Rayleigh number. *Physical Review A*, 46(8):4742–4754, Oct 1992. doi: 10.1103/physreva.46.4742.
- [3] J. Kenji López-Alt. The Food Lab: Flip your steaks multiple times for better results. <https://www.serious eats.com/2013/07/the-food-lab-flip-your-steaks-and-burgers-multiple-times-for-better-results>. July 2013. Retrieved 2019-02-25.
- [4] A. J. T. M. Mathijssen, M. Lisicki, V. N. Prakash, and E. J. L. Mossige. Culinary fluid mechanics and other currents in food science, 2022. <https://arxiv.org/abs/2201.12128>.
- [5] D. Ou and G. S. Mittal. Single-sided pan frying of frozen hamburgers with flippings for microbial safety using modeling and simulation. *J. Food Eng.*, 80:33–45, May 2007. doi: 10.1016/j.jfoodeng.2006.03.033.
- [6] M. A. Pinsky. *Partial differential equations and boundary-value problems with applications*. American Mathematical Society, Providence, RI, third edition, 2011.

- [7] R. Stroshine. Physical properties of agricultural materials and food products. Course Manual, Purdue University, West Lafayette, IN, 1998.
- [8] J.-L. Thiffeault. Using multiscale norms to quantify mixing and transport. *Nonlinearity*, 25(2):R1–R44, February 2012. doi: 10.1088/0951-7715/25/2/R1.
- [9] J.-L. Thiffeault and G. A. Pavliotis. Optimizing the source distribution in fluid mixing. *Physica D*, 237(7):918–929, June 2008. doi: 10.1016/j.physd.2007.11.013.
- [10] J. Zhang, S. Childress, and A. Libchaber. Non-Boussinesq effect: Thermal convection with broken symmetry. *Physics of Fluids*, 9(4):1034–1042, April 1997. doi: 10.1063/1.869198.
- [11] S. E. Zorrilla and R. P. Singh. Heat transfer in double-sided cooking of meat patties considering two-dimensional geometry and radial shrinkage. *J. Food Eng.*, 57:57–65, 2003.

### A. Boundary layer solution for symmetric problem

The fixed-point profile in the symmetric case is given by Eq. (6.7):

$$U_{\Delta t}(z) = \frac{1}{2} + \sum_{m \text{ even}} \tanh(\mu_m^2 \Delta t / 2) \hat{S}_m \phi_m(z). \quad (\text{A.1})$$

In this Appendix we find the boundary layer structure of  $U_{\Delta t}(z)$  in the rapid-flipping limit  $\Delta t \rightarrow 0$ , for the case of perfect conductors  $h_0 = h_1 = \infty$ , for which

$$\mu_m = m\pi, \quad \phi_m(z) = \sqrt{2} \sin m\pi z, \quad \hat{S}_m = \frac{\sqrt{2}}{\pi m}. \quad (\text{A.2})$$

Define the stretched variables  $Z = z/\sqrt{\Delta t}$  and  $k_m = \mu_m \sqrt{\Delta t}$ ; Eq. (A.1) is then

$$U_{\Delta t}(Z\Delta t) = \frac{1}{2} + \sum_{m \text{ even}} \tanh(k_m^2 / 2) \frac{\sin(k_m Z)}{\pi k_m} \Delta k_m \quad (\text{A.3})$$

where  $\Delta k_m = k_{m+2} - k_m = 2\pi\sqrt{\Delta t}$ . In the limit  $\Delta t \rightarrow 0$  the sum (A.3) becomes the integral

$$\lim_{\Delta t \rightarrow 0} U_{\Delta t}(Z\Delta t) =: U(Z) = \frac{1}{2} + \int_0^\infty \tanh(k^2 / 2) \frac{\sin(kZ)}{\pi k} dk. \quad (\text{A.4})$$

This is convergent at  $k = 0$  and  $k = \infty$ , but for large  $k$  it only converges because the fast oscillations of  $\sin(kZ)$  overcome the slow decay  $1/k$ . To improve convergence, first note that

$$\int_0^\infty \frac{\sin(kZ)}{\pi k} dk = \frac{1}{\pi} \int_0^\infty \frac{\sin x}{x} dx = \frac{1}{2}, \quad Z > 0. \quad (\text{A.5})$$

We then add and subtract 1 in the integrand of Eq. (A.4) to get

$$\begin{aligned} U(Z) &= 1 + \int_0^\infty (\tanh(k^2 / 2) - 1) \frac{\sin(kZ)}{\pi k} dk \\ &= 1 - \frac{2}{\pi} \int_0^\infty \frac{1}{1 + e^{k^2}} \frac{\sin(kZ)}{k} dk. \end{aligned} \quad (\text{A.6})$$

Now the integrand converges exponentially for large  $k$ , making numerical integration much easier. Figure A.11 shows essentially perfect agreement between Eqs. (A.1) and (A.6) for  $\Delta t = 0.001$ .<sup>12</sup>

It's possible to evaluate the integral in (A.6) using contour integration to obtain

$$U(Z) = \frac{1}{2} + \sum_{n > 0 \text{ odd}} \frac{2}{\pi n} e^{-Z\sqrt{n\pi/2}} \sin(Z\sqrt{n\pi/2}). \quad (\text{A.7})$$

However, the sum in (A.7) is very poorly convergent for small  $Z$ , and so numerical integration of (A.6) is actually easier in that case. Keeping one term in the sum, we can easily show that the overshoot in the boundary layer solution is near  $Z = \sqrt{25\pi/8} \approx 3.13329$  (exact value 3.12875...).

<sup>12</sup>The MATLAB function `flipheatbl` computes the boundary layer solution in Fig. A.11.

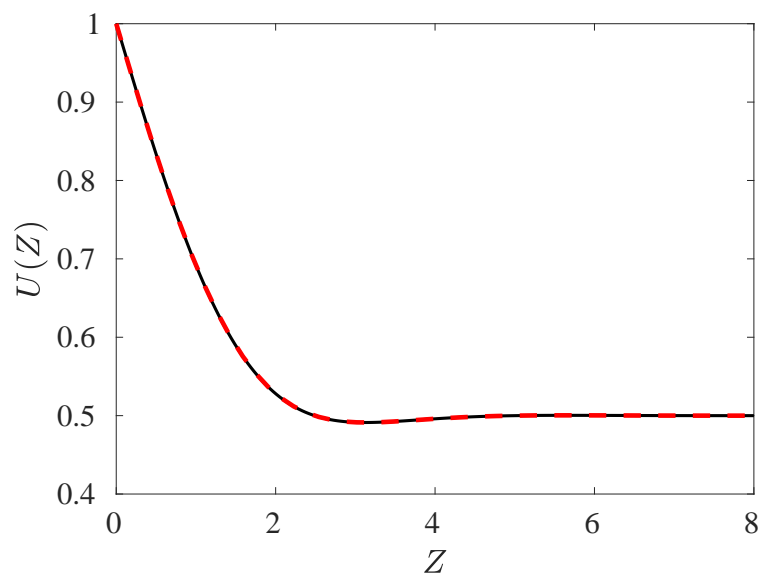


Figure A.11: Boundary layer solution from numerical evaluation of Eq. (A.6) (solid) and from the sum Eq. (A.1) for  $\Delta t = 0.001$  (dashed).